

Photovoltaic Properties of a Conjugated Polymer Blend of MDMO–PPV and PCNEPV

S. C. Veenstra,^{*,†} W. J. H. Verhees,[†] J. M. Kroon,[†] M. M. Koetse,[‡] J. Sweelssen,[‡]
J. J. A. M. Bastiaansen,[‡] H. F. M. Schoo,[‡] X. Yang,[§] A. Alexeev,[§] J. Loos,[§]
U. S. Schubert,[§] and M. M. Wienk^{||}

Energy Research Centre of The Netherlands (ECN), P.O. Box 1, 1755 ZG,
Petten, The Netherlands, TNO Industrial Technology, Eindhoven, The Netherlands,
Laboratory of Polymer Technology and Laboratory of Macromolecular Chemistry and
Nanotechnology, Eindhoven University of Technology, Eindhoven, The Netherlands

Received January 14, 2004. Revised Manuscript Received April 2, 2004

Photovoltaic properties of solution-processed semiconducting polymer blends have been studied. It is demonstrated that photoinduced charge transfer occurs in binary mixtures of poly[2-methoxy-5-(3,7-dimethyloctyloxy)-1,4-phenylenevinylene] (MDMO–PPV) and poly[oxa-1,4-phenylene-(1-cyano-1,2-vinylene)–(2-methoxy-5-(3,7-dimethyloctyloxy)-1,4-phenylene)-1,2-(2-cyanovinylene)-1,4-phenylene] (PCNEPV). Further, it is shown that the photovoltaic performance is improved by a thermal treatment which alters the morphology of the photoactive layer. The temperature necessary to achieve the enhanced performance is related to transition temperatures of the pure polymers. Device optimization yields solar cells with a power conversion efficiency of 0.75% under standard test conditions (AM 1.5, 1000 W/m²).

Introduction

The discovery of photoinduced charge transfer in composites of conjugated polymers and C₆₀ initiated a strong research effort toward exploitation of this process as an efficient charge-generation step in organic photovoltaic devices with the aim of fabricating low-cost solar cells.^{1–3} Early devices yielded maximum external quantum efficiencies (or electrons collected per incident photon, IPCE) of around 9%. This was increased by a factor of 3 by improving the miscibility of the fullerene derivative with the conjugated polymer, thus forming a so-called bulk heterojunction.⁴ Further optimization has recently led to polymer/fullerene-based devices with IPCEs up to 76% and power efficiencies of 3% under simulated solar light (AM 1.5, 1000 W/m²).^{5,6}

Inspired by these developments, similar systems were examined such as blends of two conjugated polymers and hybrid systems containing a conjugated polymer and inorganic semiconductors.^{7–16} However, these latter two concepts received considerably less attention over

the past decade, although all three systems have the potential to be implemented in consumer electronics and inexpensive, large-area photovoltaic systems.^{17,18}

This paper focuses on photovoltaic devices based on a blend of two conjugated polymers: a dialkoxy substituted poly(*para*-phenylenevinylene) derivative (MDMO–PPV) as electron donor and poly[oxa-1,4-phenylene-(1-cyano-1,2-vinylene)–(2-methoxy-5-(3,7-dimethyloctyloxy)-1,4-phenylene)-1,2-(2-cyanovinylene)-1,4-phenylene] (PCNEPV) as electron acceptor. The chemical structures of the polymers are presented in the inset of Figure 1. It was shown by Carter and co-workers that a similar mixture is potentially interesting for photovoltaic applications.¹⁹ Several derivatives of the two

* Corresponding author. E-mail: veenstra@ecn.nl.

[†] Energy Research Centre of The Netherlands.

[‡] TNO Industrial Technology.

[§] Laboratory of Polymer Technology, Eindhoven University of Technology.

^{||} Laboratory of Macromolecular Chemistry and Nanotechnology, Eindhoven University of Technology.

(1) Sariciftci, N. S.; Smilowitz, L.; Heeger, A. J.; Wudl, F. *Science* **1992**, *258*, 1474.

(2) Sariciftci, N. S.; Heeger, A. J. *Int. J. Mod. Phys. B* **1994**, *8*, 237.

(3) Halls, J. J. M.; Pichler, K.; Friend, R. H.; Moratti, S. C.; Holmes, A. B. *Appl. Phys. Lett.* **1996**, *68*, 3120.

(4) Yu, G.; Gao, J.; Hummelen, J. C.; Wudl, F.; Heeger, A. J. *Science* **1995**, *270*, 1789.

(5) Schilinsky, P.; Waldauf, C.; Brabec, C. J. *Appl. Phys. Lett.* **2002**, *81*, 3885.

(6) Wienk, M. M.; Kroon, J. M.; Verhees, W. J. H.; Knol, J.; Hummelen, J. C.; van Hal, P. A.; Janssen, R. A. J. *Angew. Chem., Int. Ed.* **2003**, *42*, 3371.

(7) Halls, J. J. M.; Walsh, C. A.; Greenham, N. C.; Marseglia, E. A.; Friend, R. H.; Moratti, S. C.; Holmes, A. B. *Nature* **1995**, *376*, 498.

(8) Yu, G.; Heeger, A. J. *J. Appl. Phys.* **1995**, *78*, 4510.

(9) Arias, A. C.; MacKenzie, J. D.; Stevenson, R.; Halls, J. J. M.; Inbasekaran, M.; Woo, E. P.; Richards, D.; Friend, R. H. *Macromolecules* **2001**, *34*, 6005.

(10) Jonforsen, M.; Ahmad, I.; Johansson, T.; Larsson, J.; Roman, L. S.; Svensson, M.; Inganäs, O.; Andersson, M. R. *Synth. Met.* **2001**, *119*, 185.

(11) Zhang, F.; Jonforsen, M.; Johansson, D. M.; Andersson, M. R.; Inganäs, O. *Synth. Met.* **2003**, *138*, 555.

(12) Granström, M.; Petritsch, K.; Arias, A. C.; Lux, A.; Andersson, M. R.; Friend, R. H. *Nature* **1998**, *395*, 257.

(13) Arango, A. C.; Johnson, L. R.; Bliznyuk, V. N.; Schlesinger, Z.; Carter, S. A.; Hörhold, H.-H. *Adv. Mater.* **2000**, *12*, 1689.

(14) Huynh, W. U.; Dittmer, J. J.; Alivisatos, A. P. *Science* **2002**, *295*, 2425.

(15) van Hal, P. A.; Wienk, M. M.; Kroon, J. M.; Verhees, W. J. H.; Slooff, L. H.; van Gennip, W. J. H.; Jonkheijm, P.; Janssen, R. A. J. *Adv. Mater.* **2003**, *15*, 118.

(16) Coakley, K. M.; Liu, Y.; McGehee, M. D.; Frindell, K. L.; Stucky, G. D. *Adv. Funct. Mater.* **2003**, *13*, 301.

(17) Padinger, F.; Brabec, C. J.; Fromherz, T.; Hummelen, J. C.; Sariciftci, N. S. *Opto-Electr. Rev.* **2000**, *8*, 280.

(18) Brabec, C. J.; Padinger, F.; Hummelen, J. C.; Janssen, R. A. J.; Sariciftci, N. S. *Synth. Met.* **1999**, *102*, 861.

(19) Chasteen, S.; Carter, S. A.; Tillmann, H.; Hörhold, H.-H. Poster Presentation, SPIE Conference, Seattle, WA, 2002; no. 4801.

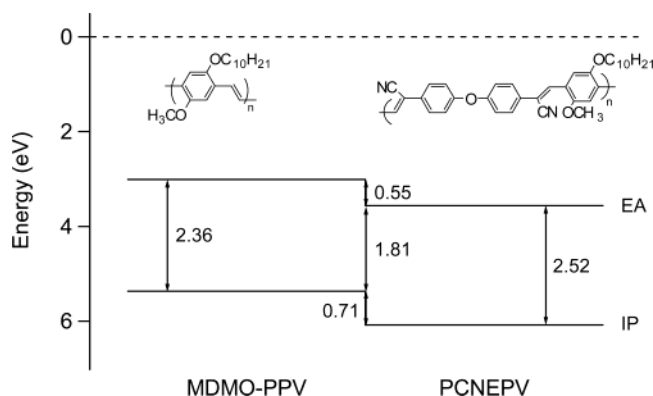


Figure 1. Electron affinities (EA) and ionization potentials (IP) of MDMO-PPV (2.97 and 5.33 eV, respectively) and PCNEPV (3.52 and 6.04 eV, respectively). Values determined by cyclic voltammetry from the onset of the oxidation (0.63 and 1.34 V) and reduction peaks (−1.73 V and −1.18 V for MDMO-PPV and PCNEPV, respectively) vs SCE and converted to values relative to the vacuum level. The inset shows the chemical structure of MDMO-PPV (left) and PCNEPV (right), OC₁₀H₂₁ abbreviates for 3,7-dimethyloctyloxy side chains.

components were synthesized, and here we describe the photovoltaic properties of blends of polymers containing 2-methoxy-5-(3,7-dimethyloctyloxy) (MDMO) side chains. These polymers are similar to the polymers used in the first polymer-blend-based photovoltaic devices, the major difference being the ether bond in the backbone of the electron-accepting polymer.^{7,8}

The maximum IPCE of polymer blend devices obtained so far is generally less than 10%.^{7–11} This is commonly attributed to several factors, such as the short exciton diffusion length of conjugated polymers relative to the typical domain sizes in polymer/polymer blends, the low charge carrier mobilities, and the lack of stable conjugated polymers with a high electron affinity. Higher quantum efficiencies (~29%) have been reported for laminated photovoltaic devices, however these cells are inherently difficult to process.¹²

The polymer blend studied here is easily processed and shows maximum IPCEs of 8–10%. We found that maximum IPCE values of around 23% could be achieved by optimizing the device structure in combination with a thermal treatment. This led to polymer-based photovoltaic devices with an AM 1.5 (1000 W/m²) power conversion efficiency of 0.75%.

Experimental Section

As electron donor poly[2-methoxy-5-(3,7-dimethyloctyloxy)-1,4-phenylenevinylene] (MDMO-PPV) is used. The material was synthesized using the sulfinyl route,²⁰ yielding a weight average molecular weight (M_w) of 570×10^3 g/mol with a polydispersity index of 5.

PCNEPV is used as electron acceptor. PCNEPV is an acronym for poly[oxa-1,4-phenylene-1,2-(1-cyanovinylene)-(2-methoxy-5-(3,7-dimethyloctyloxy)-1,4-phenylene)-1,2-(2-cyanovinylene)-1,4-phenylene]. Three batches differing in molecular weight were synthesized as described elsewhere.^{21,22} The

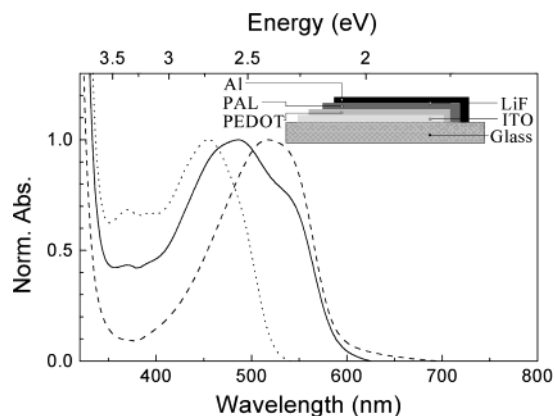


Figure 2. Normalized absorption spectra of thin films spin coated on glass of MDMO-PPV (dashed line), PCNEPV (dotted line), and a 1:1 blend (by weight) of both polymers (continuous line). The inset gives a schematic, cross-sectional view of a typical device. PAL stands for photoactive layer. See Experimental Section for further details.

PCNEPV polymers were end-capped with benzyloxy or diethyl-benzylphosphonate. The polymers were analyzed with ¹H NMR and FTIR giving spectra confirming the desired products. The weight-average molecular weights (M_w s) of the batches were 3.5×10^3 , 47×10^3 , and 113.5×10^3 g/mol, with polydispersity indexes of 1.7, 4.8, and 2.8, respectively. The M_w and polydispersity indexes were measured against poly(styrene) standards. For all measurements we used the intermediate molecular weight PCNEPV batch unless stated otherwise.

To study the photovoltaic performance of devices based on a blend of these two conjugated polymers, a large number of devices were produced using an approach similar to that previously reported.^{23,24} Glass substrates were used with pre-patterned ITO electrodes that were generously provided by Philips Research. These transparent front electrodes were carefully cleaned, dried, and treated with O₃ prior to use. On the substrates, layers of ~60 nm of PEDOT:PSS (Baytron-P, Bayer) were spin coated. The photoactive layers were spun from chlorobenzene (SigmaAldrich, HPLC-grade) solutions of the polymer mixture. Typically, we used solutions containing 0.25 wt % of either polymer. The spin-coating conditions were adjusted to give photoactive layers between 30 and 65 nm.²⁵ Finally, a 1-nm layer of LiF (Sigma Aldrich) and 80 nm of Al (5 N, Sigma Aldrich) were evaporated at $1 \cdot 10^{-6}$ mbar through a shadow mask. In this way, 4 cells were obtained with areas of 0.10 cm², 0.17 cm², 0.37 cm², and 1.0 cm² on the same substrate. A schematic cross-sectional view of a device is given in the inset of Figure 2. Film thickness measurements were performed with a Dektak 8 surface profilometer (Veeco).

Electrical device characterization and annealing experiments were performed under a N₂ atmosphere. Samples were cooled by placing them on a steel plate (at room temperature) giving a cooling rate of 10 °C/min. Current density–voltage (J/V) tests were carried out using a home-built setup with a tungsten/halogen lamp (12 V/50 W) and a Keithley SMU 2400. For spectral response measurements the same setup was used in combination with a set of 22 interference filters, without bias light. The response of the samples was calculated relative to the response of a calibrated Si-diode. From the overlap of the spectral response of the sample with the standard AM 1.5 (1000 W/m²) spectrum we calculated the short circuit current density under AM 1.5 conditions ($J_{sc,SR}$) assuming a linear

(20) Lutsen, L.; Adriaensens, P.; Becker, H.; van Breemen, A. J.; Vanderzande, D.; Gelan, J. *Macromolecules* **1999**, *32*, 6517.

(21) Tillman, H.; Hörhold, H.-H. *Synth. Met.* **1999**, *101*, 138.

(22) Koetse, M. M.; Sweelssen, J.; Franse, T.; Veenstra, S. C.; Kroon, J. M.; Yang, X.; Alexeev, A.; Loos, J.; Schubert, U. S.; Schoo, H. F. M. *Proc. SPIE-Int. Soc. Opt. Eng.* **2004**, 5215, (Organic Photovoltaics IV) 119.

(23) Katz, E. A.; Faiman, D.; Tuladhar, S. M.; Kroon, J. M.; Brabec, C. J.; Sariciftci, N. S. *J. Appl. Phys.* **2001**, *90*, 5343.

(24) Shaheen, S. E.; Brabec, C. J.; Sariciftci, N. S.; Padinger, F.; Fromherz, T.; Hummelen, J. C. *Appl. Phys. Lett.* **2001**, *78*, 841.

(25) We note that the photovoltaic properties of annealed devices with the structure ITO/PEDOT/MDMO-PPV:PCNEPV(1:1)/PCNEPV/LiF/Al are only weakly dependent on the total thickness of the photoactive layers within the given range (30–65 nm).

relation between the illumination intensity and the short circuit current density. The $J_{sc,SR}$ is in this way largely insensitive to aging of tungsten/halogen lamp and (long term) intensity variations. The fill factor (FF), maximum power point (MPP), mismatch factor, and the power conversion efficiency (η_e) were determined using standard definitions.²⁶ A Spectrolab XT-10 solar simulator was used to measure the power conversion efficiency under standard test conditions (AM 1.5, 1000 W/m²) in air. The particular combination of the spectral response of the test and calibrated reference cell together with the spectrum of the solar simulator and the tabulated AM 1.5 spectrum resulted in a mismatch factor of 0.87. The active area of the test cell was 0.17 cm², and the thickness of the photoactive layer was 45 nm. The sample was annealed at 80 °C for 10 min.

For annealing purposes, the devices were placed on a hotplate giving the desired temperature within ± 2 °C, as confirmed by a dummy cell equipped with a thermocouple.

Electrochemical (cyclic voltammetry, CV) measurements were performed with a Potentiostat Wenking POS73 potentiostat. Both the working electrode and the counter electrode were of platinum. A saturated calomel electrode (SCE), calibrated against a Fc/Fc⁺ couple, was used as reference electrode. The measurements were conducted in dichloromethane solutions (1 mg/mL) with 0.1 M tetrabutylammonium hexafluorophosphate as supporting electrolyte. The onset of the reduction (E_{red}) and oxidation (E_{ox}) waves were used to estimate the electron affinity (EA) and the ionization potential (IP) by the relation $EA = E_{red} + 4.7$ and $IP = E_{ox} + 4.7$, respectively.

Samples for optical (absorption and emission) and morphological (AFM and TEM) measurements were prepared by spin coating under conditions comparable to those used for device fabrication. UV-Vis absorption spectra of thin polymer films on glass substrates were recorded on a Perkin-Elmer Lambda 900 UV-Vis-near-IR spectrometer. Time-integrated emission spectra were obtained with an Edinburgh Instruments LifeSpec-PS spectrometer with a Hamamatsu microchannel plate photomultiplier.

Atomic force microscopy (AFM) measurements were performed with a Solver P74H for high-temperature measurements (NT-MDT Co., Russia). Samples were prepared by spin coating on a PEDOT/PSS layer, followed by floating off the active layer in water, after which it was transferred to mica. Both the top and bottom sides of the layers were probed.

Samples for transmission electron microscopy (TEM) were transferred to a 400-mesh copper TEM grid after float-off. The TEM measurements were conducted on a JEOL JEM-2000FX transmission electron microscope operated at 80 kV.

DSC measurements were performed with a Perkin-Elmer DSC7 differential scanning calorimeter equipped with an autosampler. Scans were made between 0 and 250 °C with a heating and cooling rate of 20 °C/min in a nitrogen atmosphere. No degradation of the polymers was observed over this temperature range.

Results and Discussion

For organic photovoltaic devices based on a donor-acceptor system, the mutual alignment of the frontier orbitals is of crucial importance, as it determines whether the photoinduced charge transfer is thermodynamically allowed. To gain insight into these energy levels we used cyclic voltammetry to estimate the electron affinity and the ionization potential of MDMO-PPV and PCNEPV. Figure 1 presents the results.

From Figure 1 one can infer that MDMO-PPV and PCNEPV form a donor-acceptor pair. The energy difference between the electron affinity of PCNEPV and

MDMO-PPV is 0.55 eV. This step in energy levels provides a driving force for (photoinduced) charge transfer. Another process that may occur in donor-acceptor systems is energy transfer.

Halls et al. studied two donor-acceptor blends consisting of PPV-based polymers.²⁷ One system was based on a blend of DMOS-PPV with CN-PPV, and showed energy transfer upon optical excitation. The other system, composed of MEH-PPV with CN-PPV, gave charge transfer. To account for these observations, the authors proposed a model based on the energy of the lowest optical excitations, the mutual alignment of the frontier orbitals of these polymers, and a term similar to an exciton binding energy. When we apply this model to the system presented here and assume that the difference in electron affinities is similar to the difference in LUMO levels, we find that the lowest electronic excitation is an intermolecular excitation, about 0.2 eV below the lowest intramolecular excitation. From this we expect that we may find photoinduced charge transfer in MDMO-PPV:PCNEPV blends.²⁸

Figure 2 shows normalized UV-Vis absorption spectra for thin films of MDMO-PPV (dashed line) and PCNEPV (dotted line). The spectrum of the blend, also presented in Figure 2 (blend ratio 1:1, continuous line), is a superposition of both components constituting the blend. This shows that charge transfer is insignificant in the ground state of the polymer composite, as expected from the energy diagram presented in Figure 1.

The long wavelength absorption maxima in the spectra, at 518 nm for MDMO-PPV and 455 nm for PCNEPV, correspond to the characteristic $\pi-\pi^*$ transitions in conjugated polymers. After photoexcitation, the polymer returns either to the ground state by radiative or nonradiative decay or to a charge separated state. Figure 3 shows the time-integrated photoluminescence spectra of the pure polymer films, together with two polymer blends (blend ratio 1:1). The spectra are normalized to the optical density of the film at the excitation wavelength (480 nm) and to the integration time, and, in the case of MDMO-PPV, multiplied by a scaling factor. PCNEPV is a highly luminescent material giving the highest response with a broad and featureless emission spectrum ranging from 500 to 700 nm and a maximum at 564 nm. The fluorescence maximum of the MDMO-PPV film (at 583 nm) is a factor of 7.5 lower as compared to PCNEPV, and reveals a shoulder at 626 nm, 0.15 eV below the maximum.

The luminescence of the polymer blend (continuous line in Figure 3) is almost quantitatively quenched, see the thin continuous line at the bottom of Figure 3. The

(27) Halls, J. J. M.; Cornil, J.; dos Santos, D. A.; Silbey, R.; Hwang, D.-H.; Brédas, J. L.; Friend, R. H. *Phys. Rev. B* **1999**, *60*, 5721.

(28) This estimate is based on a method described in ref 27. The lowest intramolecular excitation energies (E_{S1-S0}) were taken from the onsets of the optical absorption spectra (see Figure 2): 2.00 and 2.35 eV for MDMO-PPV and PCNEPV, respectively. The difference in LUMO levels (E_{ALUMO}) was estimated by taking the difference in electron affinities (0.55 eV) as determined by CV measurements (see Figure 1), thereby assuming that the difference in electron affinities is similar to the difference in LUMO levels. The (low) intermolecular excitations were estimated according to: $E_{inter} = E_{S1-S0} + E_{charge\ sep} - E_{ALUMO}$, where $E_{charge\ sep}$ stands for the energy necessary to separate the electron and the hole; the value of $E_{charge\ sep}$ is taken from ref 27 (0.35 eV). From this we estimate that the lowest intermolecular excitation is 0.2 eV below the lowest intramolecular excitation.

(26) Kroon, J. M.; Wienk, M. M.; Verhees, W. J. H.; Hummelen, J. C. *Thin Solid Films* **2002**, *403-404*, 223.

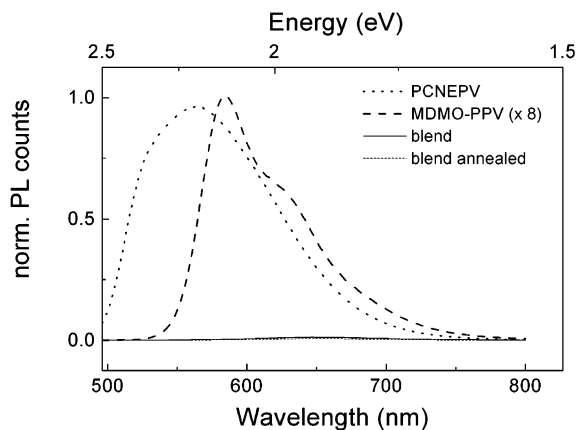


Figure 3. Photoluminescence spectra of pure films of PCNEPV (dotted line) and MDMO-PPV (dashed line) together with the spectra of films of blends, ratio 1:1 by weight, of these polymers before (continuous line) and after annealing (short dashed line). The spectra are corrected for differences in the optical densities of the films.

maximum in the luminescence spectrum of the polymer blend, found at 650 nm, is a factor of 80 lower than the luminescence maximum of PCNEPV. The dashed-dotted line represents the luminescence spectra of the polymer blend after annealing at 80 °C for 10 min. This annealing results in a slight reduction of the remaining luminescence.

The strong quenching of the photoluminescence in the polymer blend supports the expected photoinduced charge transfer as the intermolecular (charged) excitation was estimated to be 0.2 eV below the lowest intramolecular excitation. From the observed efficient photoluminescence quenching in the polymer blend, we infer that the majority of the excitons reach the donor-acceptor interface where they are separated into charges located on either side of the polymer interface: holes in the MDMO-PPV phase and electrons in the PCNEPV phase. This implies that the exciton diffusion length is at least of the same order of magnitude as the average distance between both polymer phases. The exciton diffusion length of PPV polymers is around 8–20 nm.^{1,29,30} Because the total thickness of the blend layer is 30–40 nm, we cannot conclude from this that a bulk heterojunction is formed: a bilayer structure with a relatively long exciton diffusion length, possibly combined with a rough interface, could also give rise to the observed photoluminescence quenching. However, the combination of efficient photoluminescence quenching and the high external quantum efficiency (as shown below) shows that photoinduced charge transfer occurs in this donor-acceptor system.

To learn more about the morphology of the polymer blends we studied the sample microstructure by scanning probe and electron microscopy techniques. AFM measurements carried out on the top-side of pristine polymer blend films showed a flat surface, with an rms roughness of about 2 nm. No clear phase separation was observed in either topography or phase contrast mode. Sample annealing did not induce any changes in these

observations. From this we conclude that the phase separation either occurs below the detection limit of our AFM device or occurs laterally resulting in the formation of a double layerlike system.

To assess information on the interface between PEDOT and the MDMO-PPV:PCNEPV layer, a float-off technique was used to remove the polymer layers from the glass/ITO substrate. By doing so, the PEDOT layer dissolved and the photoactive layer floated on the water. It is assumed that this procedure does not alter the morphology of the active layer. The backside of the pristine polymer blend film was surprisingly rough, patterns in the form of a network and droplets were found (Figure 4a). This structure is attributed to dewetting of the photoactive blend on top of the PEDOT layer. To rule out the presence of PEDOT left after floating, we also probed films that were peeled from the substrate, and these surfaces yielded similar AFM images. Further, we note that the spin-coated PEDOT:PSS layer is flat (rms roughness <2 nm) and consequently does not act as a mold for the observed rough layer. The height of the structures is about 12 nm, which is considerable compared to the ~40-nm thickness of the measured film.

The backsides of *annealed* films (on PEDOT:PSS) were completely flat (rms roughness < 2 nm). Moreover, temperature-dependent AFM experiments on (initially pristine) films revealed the disappearance of the structure at 70 °C. Blends spun on bare glass substrates do not show this behavior and form flat films. The same holds for films of the pure materials on either PEDOT or glass.

The structure found in pristine films of MDMO-PPV:PCNEPV blends prevented us from using TEM as a tool to study phase separation in these films. The reason for this is that both the sample roughness and compositional variations cause contrast in TEM imaging. We therefore studied TEM images of the flat, annealed films. Detailed electron microscopy studies on MDMO-PPV:PCNEPV blends using a transmission microscope equipped with an electron energy loss spectroscopy setup revealed that the dark spots in the bright field image, presented in Figure 4b, correspond to N-rich domains and are thus related to phases with a high concentration of PCNEPV.³¹ From this, we conclude that phase separation is found in annealed films of MDMO-PPV:PCNEPV blends. The typical domain sizes of the donor-acceptor blend, 20–50 nm, are close to the exciton diffusion length in PPV-based polymers and therefore suitable for charge separation.

Both the photoluminescence quenching and the morphology measurements already showed that annealing influenced the optical and structural properties of the polymer blend. The relation between the anneal temperature and the spectral response was investigated by fabricating a large number of devices which were annealed for 10–15 min at different temperatures.³²

(31) Loos, J.; Yang, X.; Koetse, M. M.; Sweelssen, J.; Schoo, H. F. M.; Veenstra, S. C.; Grogger, W.; Kothleitner, G.; Hofer, F. Submitted for publication.

(32) The effect of the anneal time on the spectral response of devices was determined. Ten samples (with each four photovoltaic devices) with the polymer blend containing the intermediate-molecular-weight PCNEPV were annealed at 90 °C with annealing times ranging between 180 s and 14 h. The calculated AM 1.5 short circuit currents were identical within the measurement error.

(29) Savenije, T. J.; Warman, J. M.; Goossens, A. *Chem. Phys.* **1998**, *287*, 148.

(30) Vacar, D.; Maniloff, E. S.; McBranch, D. W.; Heeger, A. J. *Phys. Rev. B* **1997**, *56*, 4573.

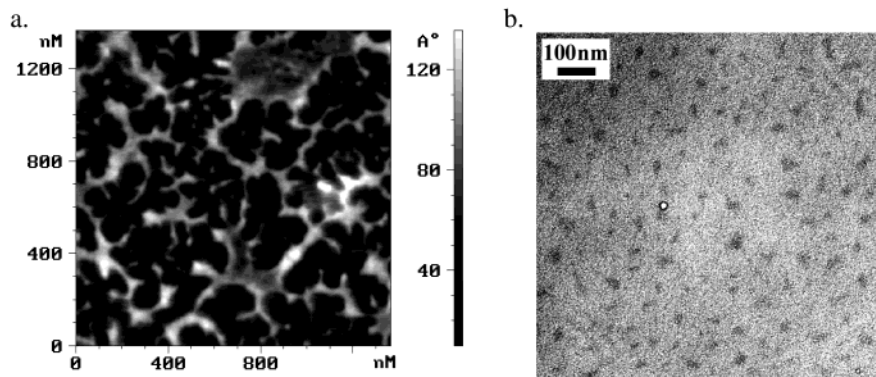


Figure 4. AFM image (height contrast, $1.4 \times 1.4 \mu\text{m}$; vertical scale, 120 \AA) of the bottom side of an MDMO-PPV/PCNEPV blend (1:1 ratio) before annealing (a). Energy-filtered TEM image (zero-loss filtered) of an MDMO-PPV/PCNEPV (1:1 blend) after annealing; the scale bar indicates 100 nm (b).

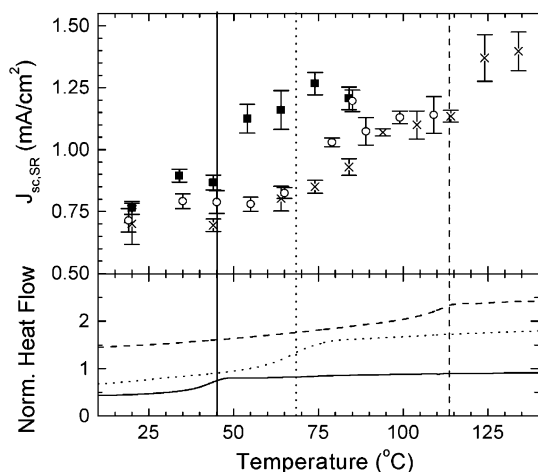


Figure 5. Top panel shows the calculated AM 1.5 current density at 1000 W/m^2 ($J_{\text{sc,SR}}$), as calculated from the spectral response of the sample, as a function of the sample anneal temperature for three types of polymer blends differing in the molecular weight (M_w) of the PCNEPV polymer: full squares represent the values obtained with a blend containing the low- M_w PCNEPV, open circles represent the intermediate- M_w PCNEPV, and crosses represent the high- M_w PCNEPV. The lower panel shows the differential scanning calorimetry (DSC) scan of the three PCNEPV batches: the full line shows the scan of the low- M_w PCNEPV, the dotted line shows the scan of the intermediate- M_w PCNEPV, and the dashed line is the scan on the high- M_w PCNEPV. The vertical lines are a guide for the eye.

The spectral response of each device was recorded after the sample reached room temperature. Next, the short-circuit current density of the device under AM 1.5 conditions ($J_{\text{sc,SR}}$) was calculated from the overlap of the spectral response with a standard solar spectrum (AM 1.5, 1000 W/m^2), assuming a linear relation between the illumination intensity and the photocurrent. Samples were prepared using one batch of MDMO-PPV and three different batches of PCNEPV with weight-average molecular weights (M_w) of $3.5 \times 10^3 \text{ g/mol}$ (full squares), $47 \times 10^3 \text{ g/mol}$ (open circles), and $113 \times 10^3 \text{ g/mol}$ (crosses). The results are summarized in the top panel of Figure 5.

First, the devices prepared with a blend containing the low-molecular-weight PCNEPV (black squares) are discussed. The short-circuit current densities of these

devices are around 0.85 mA/cm^2 for temperatures between 20 and $45 \text{ }^\circ\text{C}$. Samples annealed at temperatures above $55 \text{ }^\circ\text{C}$ give higher current densities of about 1.2 mA/cm^2 . A similar trend was obtained for devices prepared with the intermediate-molecular-weight PCNEPV (open circles), only the transition to higher short circuit current densities is shifted to higher temperatures: i.e., between 65 and $80 \text{ }^\circ\text{C}$. The high-molecular-weight PCNEPV derivative shows a more complex behavior with a gradual increase in short circuit current density between 70 and $90 \text{ }^\circ\text{C}$ followed by a sharp transition between 115 and $125 \text{ }^\circ\text{C}$.

Generally, the morphology of a polymer film is “frozen” below the glass transition temperature (T_g). To accommodate a morphological change within a reasonable time scale, the temperature of the sample should be close to or above the T_g of at least one of the polymers in the composite. The differential scanning calorimetry (DSC) scans of the three PCNEPV derivatives is presented in the lower panel of Figure 5. The lowest trace was recorded on the low-molecular-weight PCNEPV derivative. The transition in this DSC scan is found at around $45 \text{ }^\circ\text{C}$; close to the transition observed in the short circuit current density of the blend based on the same PCNEPV. For the intermediate-molecular-weight PCNEPV both transitions (T_g and $J_{\text{sc,SR}}$) coincide around $70 \text{ }^\circ\text{C}$. The DSC trace of the high-molecular-weight PCNEPV (top trace in lower panel of Figure 5) gives a transition around $115 \text{ }^\circ\text{C}$, corresponding to the high-temperature transition in the current density plot. We therefore expect that the gradual increase in short circuit current density found around $80 \text{ }^\circ\text{C}$ is related to a transition in MDMO-PPV. This was indeed confirmed by thermal dynamic mechanical analysis (DMTA) on the MDMO-PPV used in these experiments which showed a broad transition around $80 \text{ }^\circ\text{C}$. This transition is tentatively attributed to melting of the side chains. We note that the temperature-dependent AFM measurements support the notion that the sample morphology changes when the sample (with the intermediate-molecular-weight PCNEPV-derivative) is annealed above $70 \text{ }^\circ\text{C}$.

The removal of the layer thickness variations implies morphological changes in the polymer blend. These changes influence several key processes in the photo-

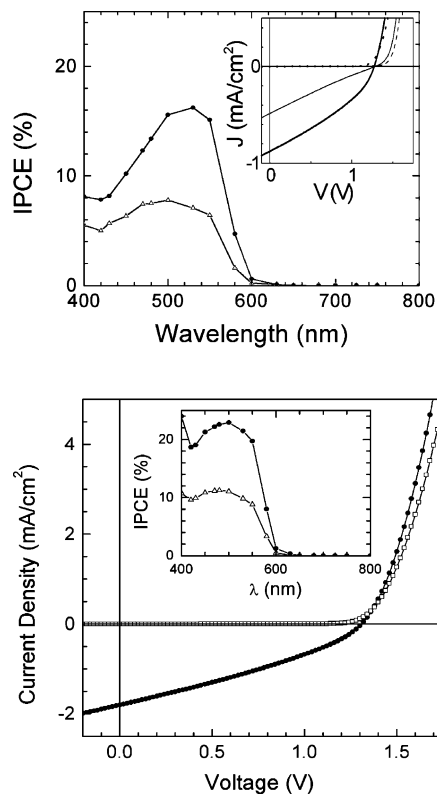


Figure 6. (a) Incident photon to charge collection efficiency (IPCE) of a typical sample consisting of a 1:1 blend of MDMO-PPV and PCNEPV, before (open symbols) and after annealing (closed symbols). The inset of the figure shows the current density-voltage characteristics with (continuous lines) and without illumination (broken lines) of a typical sample before (thin lines) and after (thick lines) an anneal treatment. (b) Current density-voltage characteristics of an optimized device (structure: ITO/PEDOT:PSS/MDMO-PPV:PCNEPV/PCNEPV/LiF/Al), measured after annealing, under standard test conditions (AM 1.5, 1000 W/m²). The inset presents the IPCE of the same device before (open symbols) and after annealing (closed symbols).

voltaic cell, such as the charge separation efficiency at the donor-acceptor interface, the charge transport process toward the electrodes, and the charge-transfer step at the electrodes. The overall effect of the anneal step leads to a strong increase in the short-circuit current. This increase is, at least in part, attributed to a better electrical contact at the PEDOT:PSS/MDMO-PPV:PCNEPV interface, thereby reducing recombination losses.

A typical plot of the current density-voltage ($J-V$) characteristic is displayed in Figure 6a. The diode was illuminated by a Tungsten halogen lamp giving an intensity of approximately 0.8 sun. Before the heat treatment, the J_{sc} is 0.45 mA/cm², the open circuit voltage (V_{oc}) is 1.38 V, and the fill factor (FF) is 22%, leading to a maximum power point (MPP) under these conditions of 0.14 mW/cm². The anneal procedure leads to an increase in J_{sc} by almost a factor of 2 (to 0.87 mA/

cm²). The FF also increases to 34%, however, the V_{oc} shows a slight decrease (to 1.28 V). This results in a MPP under these conditions of 0.38 mW/cm². A comparison between the photovoltaic properties of different PCNEPV derivatives and MDMO-PPV analogues maybe found elsewhere.²²

Devices with a slightly different structure yielded better photovoltaic performance. For example, Figure 6b gives the $J-V$ characteristics together with the IPCE of a sample (active area 0.17 cm²) made by subsequently spin coating a 1:1 blend solution onto the PEDOT/ITO substrate, followed by a pure PCNEPV solution from acetone, using in both cases the low- M_w PCNEPV. The IPCE of this sample shows relatively high values over a broad wavelength range from 400 to 550 nm with a maximum of 23% at 500 nm. This sample was measured under a class A solar simulator (see Figure 6b), yielding a short circuit current density of 1.80 mA/cm², a V_{oc} of 1.3 V, and a FF of 32%, giving a power conversion efficiency (η_e) under standard conditions (AM 1.5, 1000 W/m²) of 0.75%.

Conclusions

Polymer-based photovoltaic devices were fabricated from a blend of MDMO-PPV and PCNEPV. An energy diagram deduced from the cyclic voltammetry data indicates that photoinduced charge transfer is thermodynamically feasible in the polymer blend. Photophysical studies reveal strong photoluminescence quenching in the polymer blend. Morphological studies show that as-prepared samples have large layer thickness variations. After annealing, the roughness is removed and phase separation is identified with typical domain sizes between 20 and 50 nm.

When the photovoltaic devices are annealed above a critical temperature, the short circuit current density increases considerably. DSC measurements relate the critical anneal temperature to the T_g of the three different PCNEPV-derivatives used in this study, and to a transition in MDMO-PPV at around 80 °C. Device optimization yields polymer-based photovoltaic devices with an external quantum efficiency of 23% at 500 nm and a power conversion efficiency of 0.75%.

Acknowledgment. This work is part of the program Polymer Photovoltaics (DPI 325) of the Dutch Polymer Institute. We thank Dr. A. van Breemen and Dr. B. Langeveld (TNO, Eindhoven) for useful discussions concerning the synthesis of the polymers, I. Hovens (TNO-TPD) for performing DMTA measurements, P. Quist and Dr. T. Savenije (IRI, Delft) for performing TRMC measurements, T. Offermans and Dr. P. A. van Hal (Eindhoven University of Technology) for photophysical measurements, and Prof. Dr. R. A. J. Janssen (Eindhoven University of Technology) for fruitful discussions.

CM049917D